OSU

The Ohio State University

MOMENT METHOD ANALYSIS OF MICROSTRIP ANTENNAS OVER A WIDE FREQUENCY RANGE

B. W. Kwan and E. H. Newman

The Ohio State University

ElectroScience Laboratory

Department of Electrical Engineering
Columbus, Ohio 43212

Technical Report No. 716148-4
Grant No. NSG 1613, Supp. #8
February 1985

National Aeronautics and Space Administration
Langley Research Center
Hampton, Virginia 23665

NOTICES

When Government drawings, specifications, or other data are used for any purpose other than in connection with a definitely related Government procurement operation, the United States Government thereby incurs no responsibility nor any obligation whatsoever, and the fact that the Government may have formulated, furnished, or in any way supplied the said drawings, specifications, or other data, is not to be regarded by implication or otherwise as in any manner licensing the holder or any other person or corporation, or conveying any rights or permission to manufacture, use, or sell any patented invention that may in any way be related thereto.

50272-101

REPORT DOCUMENTATION PAGE	1. REPORT NO.	2.	3. Recipient's Accession No.
4. Title and Subtitle: MOMENT METHOD ANALYSIS OF MICROSTRIP ANTENNAS OVER A WIDE FREQUENCY RANGE			5. Report Date: February 1985 6.
7. Author(s): B. W. Kwan and E. H. Newman			8. Performing Organization Rept. No.: ESL 716148-4
9. Performing Organization Name and Address: The Ohio State University ElectroScience Laboratory Department of Electrical Engineering Columbus, Ohio 43212			10. Project/Task/Work Unit No. 11. Contract(C) or Grant(G) No. (C) (G) NSG 1613
12. Sponsoring Organization Name and Address: National Aeronautics & Space Administration Langley Research Center Hampton, Virginia 23665			13. Type of Report & Period Covered: Technical Report 14.

15. Supplementary Notes

16. Abstract (Limit: 200 words)

~~This report presents~~ ARE PRESENTED expressions for the self and mutual impedance between microstrip antenna modes on a grounded dielectric slab. The mutual impedance between the microstrip modes and a vertical current filament in the dielectric is also presented. These are the quantities required in a method of moments analysis of the microstrip antenna. Entire domain expansion modes, suitable for representing the microstrip current over a broad frequency range, are used. Efficient methods for the evaluation of the mutual impedance elements are described.

17. Document Analysis a. Descriptors

FREQ. RANGES
ANTENNA FEEDS
MICROSTRIP TRANSMISSION LINES
IMPEDANCE MATCHING
DIELECTRICS
DIPOLE CURRENT SHEETS
~~DISTRIBUTION~~ MOMENTS
COUPLED MODES
NEAR FIELDS
SUMMERFIELD APPROXIMATIONS
INTEGRALS

b. Identifiers/Open-Ended Terms

c. COSATI Field/Group

18. Availability Statement	19. Security Class (This Report): Unclassified	21. No. of Pages: 56
	20. Security Class (This Page): Unclassified	22. Price

(39.18) See Instructions on Reverse OPTIONAL FORM 272 (4-77) (Formerly NTIS-35) Department of Commerce

TABLE OF CONTENTS

LIST OF FIGURES

I. INTRODUCTION

The method of moments (MM) has proven to be an effective technique for the analysis of microstrip antennas [1-5]. Most of the previous work has concentrated on analyzing microstrip antennas near first resonance. In the method of moments analysis of the microstrip antenna the two most important quantities to be evaluated are:

1. the self or mutual impedance between the microstrip expansion and test modes which comprise the elements in the impedance matrix

2. the mutual impedance between the microstrip modes and a vertical current filament in the dielectric, representing a coaxial feed, and which comprise the elements in the right-hand side vector.

Chapter 2 finds the exact near zone fields of the microstrip modes. These fields are in terms of the Sommerfeld integrals. These fields are used to determine the mutual impedances, which are also in terms of the Sommerfeld integrals. Using the method of Pozar [6], efficient methods for the evaluation of the integrals are presented. Finally, entire domain expansion and test modes are described which would permit the analysis of the microstrip antenna over a broad frequency range.

II. PATCH DIPOLES ON A GROUNDED PLANAR DIELECTRIC SLAB

A. INTRODUCTION

To analyze the mutual coupling between patch dipole modes on a grounded dielectric slab, the electric field due to a patch dipole mode is needed. A general solution to the field equations pertaining to a microstrip patch on a grounded dielectric slab is presented in Section B. The surface current on the patch is introduced only through the boundary conditions; this simplifies the calculation, which is performed in the Fourier transform domain. The solution is essentially of the Green's function type even though the Green's function is not constructed explicitly. It is exact in the sense that both the dielectric slab and the ground plane are taken into account rigorously. Thus, surface waves and coupling to adjacent antenna elements can be accurately determined. An efficient evaluation of the Green's function is also discussed. A general expression for the mutual impedance between two rectangular patch dipoles is presented in Section C. An $e^{j\omega t}$ time dependence is assumed and suppressed throughout this chapter.

B. THEORY AND GENERAL SOLUTION

The geometry under consideration is shown in Figure 2.1. The grounded dielectric slab is infinite in extent in the x,y directions with uniform thickness t. A microstrip patch is printed on the slab at the dielectric-air interface with current density $\bar{J}_s$. Since both regions 1 and 2 are source free, an arbitrary field that satisfies

Maxwell's equations can be constructed from two scalar functions [7]: ψ_{mi} which generates a TM field and ψ_{ei} which generates a TE field, where $i = 1$ for the region inside the dielectric, and $i = 2$ for the region outside the dielectric. Both scalar functions ψ_{mi} and ψ_{ei} satisfy the scalar wave equation:

$$(\nabla^2 + k_i^2) \begin{bmatrix} \psi_{mi}(\bar{r}) \\ \psi_{ei}(\bar{r}) \end{bmatrix} = 0 \quad , \tag{2.1}$$

where $k_i^2 = \begin{cases} \epsilon_r k_o^2 & \text{in region 1} \quad (i = 1) \\ k_o^2 & \text{in region 2} \quad (i = 2) \end{cases}$,

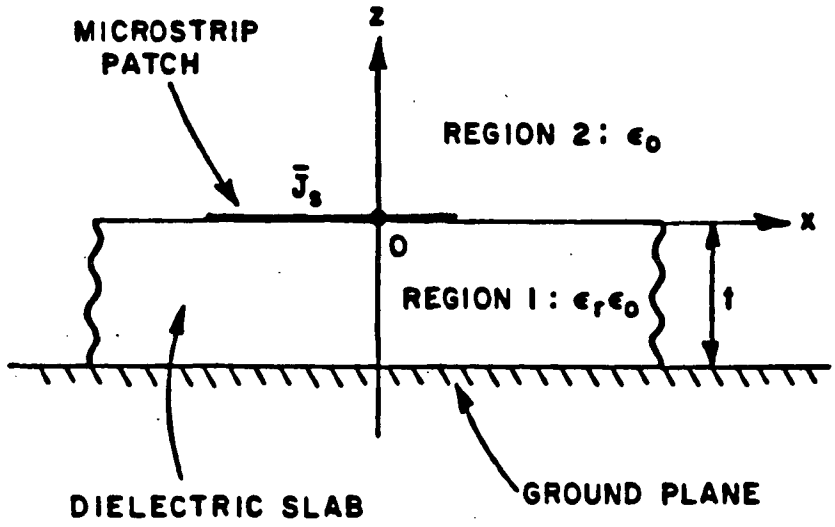

Figure 2.1. Geometry of a microstrip patch printed on a grounded dielectric slab.

k_o is the free space propagation constant, and ε_r is the relative dielectric constant in region 1.

Upon multiplying ψ_{mi} and ψ_{ei} by the unit vector $\hat{z}$, one can construct the fields as [7]

$$\bar{E}_i(\bar{r}) = -\nabla\times(\hat{z}\psi_{ei}(\bar{r})) + \frac{1}{j\omega\varepsilon_i}\nabla\times\nabla\times(\hat{z}\psi_{mi}(\bar{r})) \quad , \tag{2.2}$$

$$\bar{H}_i(\bar{r}) = \nabla\times(\hat{z}\psi_{mi}(\bar{r})) + \frac{1}{j\omega\mu_o}\nabla\times\nabla\times(\hat{z}\psi_{ei}(\bar{r})) \quad , \tag{2.3}$$

where $\varepsilon_1 = \varepsilon_r\varepsilon_o$ and $\varepsilon_2 = \varepsilon_o$. The explicit form of the field components can be found in Appendix A.

Since the structure is infinite in the x-y plane, the four scalar wave functions can be represented in terms of their spectral functions (or 2-D plane wave expansions) as follows:

in region 1

$$\begin{bmatrix} \psi_{m1}(\bar{r}) \\ \psi_{e1}(\bar{r}) \end{bmatrix} = \frac{1}{4\pi^2}\int_{-\infty}^{\infty}\int \begin{bmatrix} \tilde{\psi}_{m1}(k_x,k_y)\cos k_{z1}(z+t) \\ \tilde{\psi}_{e1}(k_x,k_y)\sin k_{z1}(z+t) \end{bmatrix} e^{-j(k_x x+k_y y)}\, dk_x dk_y \quad , \tag{2.4}$$

in region 2

$$\begin{bmatrix} \psi_{m2}(\bar{r}) \\ \psi_{e2}(\bar{r}) \end{bmatrix} = \frac{1}{4\pi^2}\int_{-\infty}^{\infty}\int \begin{bmatrix} \tilde{\psi}_{m1}(k_x,k_y) \\ \tilde{\psi}_{e1}(k_x,k_y) \end{bmatrix} e^{-j\bar{k}\cdot\bar{r}}\, dk_x dk_y \quad , \tag{2.5}$$

where

$$k_{z1} = \sqrt{\varepsilon_r k_o^2 - k_x^2 - k_y^2} \quad , \text{Re } k_{z1} > 0 \ , \text{Im } k_{z1} < 0 \ ,$$

$$k_{z2} = \sqrt{k_o^2 - k_x^2 - k_y^2} \quad , \text{Re } k_{z2} > 0 \ , \text{Im } k_{z2} < 0 \ , \tag{2.6}$$

$$\bar{k} = \hat{x}k_x + \hat{y}k_y + \hat{z}k_{z2} \quad ,$$

and

$$\bar{r} = \hat{x}x + \hat{y}y + \hat{z}z \quad .$$

It should be pointed out that using Equations (2.4,5) in (2.2,3) will automatically satisfy:

a. the boundary condition at the conducting ground plane:

$$\hat{z} \times \bar{E}_1 = 0 \quad \text{at } z = -t \quad ; \tag{2.7}$$

b. the radiation condition as $r = |\bar{r}| \to \infty$; and

c. the criterion for the integrals in (2.5) to converge as $z \to \infty$.

To specify the fields uniquely, the boundary conditions at the dielectric-air interface must be satisfied:

$$\hat{z} \times (\bar{E}_2 - \bar{E}_1) = 0 \quad \text{at } z = 0 \quad , \tag{2.8}$$

and

$$\hat{z} \times (\bar{H}_2 - \bar{H}_1) = \bar{J}_s \quad \text{at } z = 0 \quad .$$

Without loss of generality, the current density is assumed to be Fourier transformable and to have both x and y components. Hence, $\bar{J}_s$ can be written as

$$\bar{J}_s(x,y) = \hat{x}J_{sx}(x,y) + \hat{y}J_{sy}(x,y)$$

$$= \frac{1}{4\pi^2} \iint_{-\infty}^{\infty} \{\hat{x}\tilde{J}_{sx}(k_x,k_y) + \hat{y}\tilde{J}_{sy}(k_x,k_y)\} e^{-j(k_x x+k_y y)} dk_x dk_y \quad . \tag{2.10}$$

Use of Equations (2.8) and (2.9) will determine completely the spectral functions $\tilde{\psi}_{mi}, \tilde{\psi}_{ei} (i=1,2)$. The algebraic details are carried out in Appendix A. Only the field components are listed below:

region 1 ($-\infty < x,y < \infty$, $-t \leq z \leq 0$)

$$E_{x1}(\bar{r}) = \frac{j}{4\pi^2} \iint_{-\infty}^{\infty} \left[k_y \tilde{\psi}_{e1} - \frac{jk_x k_{z1}}{\omega\varepsilon_o\varepsilon_r} \tilde{\psi}_{m1} \right] e^{-j(k_x x+k_y y)} \sin k_{z1}(z+t) dk_x dk_y \quad , \tag{2.11}$$

$$E_{y1}(\bar{r}) = \frac{-j}{4\pi^2} \iint_{-\infty}^{\infty} \left[k_x \tilde{\psi}_{e1} + \frac{jk_y k_{z1}}{\omega\varepsilon_o\varepsilon_r} \tilde{\psi}_{m1} \right] e^{-j(k_x x+k_y y)} \sin k_{z1}(z+t) dk_x dk_y \quad , \tag{2.12}$$

$$E_{z1}(\bar{r}) = \frac{-j}{4\pi^2} \int\int_{-\infty}^{\infty} \frac{(k_x^2+k_y^2)}{\omega\varepsilon_o\varepsilon_r} \tilde{\psi}_{m1}\, e^{-j(k_x x+k_y y)} \cos k_{z1}(z+t)\, dk_x dk_y \quad , \tag{2.13}$$

$$H_{x1}(\bar{r}) = \frac{j}{4\pi^2} \int\int_{-\infty}^{\infty} \left[\frac{-jk_x k_{z1}}{\omega\mu_o} \tilde{\psi}_{e1} - k_y \tilde{\psi}_{m1} \right] e^{-j(k_x x+k_y y)} \cos k_{z1}(z+t)\, dk_x dk_y \quad , \tag{2.14}$$

$$H_{y1}(\bar{r}) = \frac{j}{4\pi^2} \int\int_{-\infty}^{\infty} \left[\frac{-jk_y k_{z1}}{\omega\mu_o} \tilde{\psi}_{e1} + k_x \tilde{\psi}_{m1} \right] e^{-j(k_x x+k_y y)} \cos k_{z1}(z+t)\, dk_x dk_y \quad , \tag{2.15}$$

and

$$H_{z1}(\bar{r}) = \frac{-j}{4\pi^2} \int\int_{-\infty}^{\infty} \frac{(k_x^2+k_y^2)}{\omega\mu_o} \tilde{\psi}_{e1}\, e^{-j(k_x x+k_y y)} \sin k_{z1}(z+t)\, dk_x dk_y \quad ; \tag{2.16}$$

region 2 ($-\infty < x,y < \infty$, $0 \leq z \leq \infty$)

$$E_{x2}(\bar{r}) = \frac{j}{4\pi^2} \int\int_{-\infty}^{\infty} \left[k_y\, \tilde{\psi}_{e2} + \frac{k_x k_{z2}}{\omega\varepsilon_o} \tilde{\psi}_{m2} \right] e^{-j(k_x x+k_y y+k_{z2} z)}\, dk_x dk_y \quad , \tag{2.17}$$

$$E_{y2}(\bar{r}) = \frac{-j}{4\pi^2} \iint_{-\infty}^{\infty} \left[k_x \tilde{\psi}_{e2} - \frac{k_y k_{z2}}{\omega \varepsilon_o} \tilde{\psi}_{m2} \right] e^{-j(k_x x + k_y y + k_{z2} z)} dk_x dk_y \,, \tag{2.18}$$

$$E_{z2}(\bar{r}) = \frac{-j}{4\pi^2} \iint_{-\infty}^{\infty} \frac{(k_x^2 + k_y^2)}{\omega \varepsilon_o} \tilde{\psi}_{m2} e^{-j(k_x x + k_y y + k_{z2} z)} dk_x dk_y \,, \tag{2.19}$$

$$H_{x2}(\bar{r}) = \frac{j}{4\pi^2} \iint_{-\infty}^{\infty} \left[\frac{k_x k_{z2}}{\omega \mu_o} \tilde{\psi}_{e2} - k_y \tilde{\psi}_{m2} \right] e^{-j(k_x x + k_y y + k_{z2} z)} dk_x dk_y \,, \tag{2.20}$$

$$H_{y2}(\bar{r}) = \frac{j}{4\pi^2} \iint_{-\infty}^{\infty} \left[\frac{k_y k_{z2}}{\omega \mu_o} \tilde{\psi}_{e2} + k_x \tilde{\psi}_{m2} \right] e^{-j(k_x x + k_y y + k_{z2} z)} dk_x dk_y \,, \tag{2.21}$$

and

$$H_{z2}(\bar{r}) = \frac{-j}{4\pi^2} \iint_{-\infty}^{\infty} \frac{(k_x^2 + k_y^2)}{\omega \mu_o} \tilde{\psi}_{e2} e^{-j(k_x x + k_y y + k_{z2} z)} dk_x dk_y \,, \tag{2.22}$$

where

$$\tilde{\psi}_{e1} = \frac{\omega\mu_o}{(k_x^2+k_y^2)D_e}\,[k_x\tilde{J}_{sy} - k_y\tilde{J}_{sx}] \quad , \tag{2.23}$$

$$\tilde{\psi}_{e2} = \frac{\omega\mu_o \sin k_{z1}t}{(k_x^2+k_y^2)D_e}\,[k_x\tilde{J}_{sy} - k_y\tilde{J}_{sx}] \quad , \tag{2.24}$$

$$\tilde{\psi}_{m1} = -\frac{j\epsilon_r k_{z2}}{(k_x^2+k_y^2)D_m}\,[k_x\tilde{J}_{sx} + k_y\tilde{J}_{sy}] \quad , \tag{2.25}$$

$$\tilde{\psi}_{m2} = -\frac{k_{z1}\sin k_{z1}t}{(k_x^2+k_y^2)D_m}\,[k_x\tilde{J}_{sx} + k_y\tilde{J}_{sy}] \quad , \tag{2.26}$$

$$D_e = k_{z1}\cos k_{z1}t + jk_{z2}\sin k_{z1}t \quad , \tag{2.27}$$

and

$$D_m = \epsilon_r k_{z2}\cos k_{z1}t + jk_{z1}\sin k_{z1}t \quad . \tag{2.28}$$

It should be pointed out that there are two dyadic Green's functions, $\bar{\tilde{G}}^1$ and $\bar{\tilde{G}}^2$, associated with the grounded dielectric slab. $\bar{\tilde{G}}^1$ corresponds to the case where the field points are inside the substrate (region 1), and $\bar{\tilde{G}}^2$ corresponds to the case where the field points are

outside the substrate (region 2). Only six components of each dyadic Green's function are considered since the surface current on a microstrip patch has no z-component. These components can be identified from Equations (2.11) through (2.13), and (2.17) through (2.19) as follows:

$$G^{i}_{\alpha\beta}(\bar{r},\bar{r}') = \frac{j}{\omega\mu_0} \int\int_{-\infty}^{\infty} g^{i}_{\alpha\beta}(\bar{r},k_x,k_y)\, e^{j\bar{k}\cdot\bar{r}'}\, dk_x dk_y \quad , \tag{2.29}$$

where

$i = i,2$

$\bar{k} = \hat{x}k_x + \hat{y}k_y$

$\bar{r}' = \hat{x}x' + \hat{y}y'$

$\bar{r} = \hat{x}x + \hat{y}y + \hat{z}z$

$\alpha = x,y,z$

$\beta = x,y$

and $g^{i}_{\alpha\beta}$ are obtained from the electric field components which typically have the following form:

$$E_{\alpha i}(\bar{r}) = \int\int_{-\infty}^{\infty} [g^{i}_{\alpha x}(\bar{r},k_x,k_y)\tilde{J}_{sx}(k_x,k_y) + g^{i}_{\alpha y}(\bar{r},k_x,k_y)\tilde{J}_{sy}(k_x,k_y)]dk_x dk_y . \tag{2.30}$$

It follows from Equation (2.30) that the calculations of either electric fields or mutual impedances will invariably involve the numerical evaluation of an integral of the form:

$$r = \int_{-\infty}^{\infty}\int \frac{F(k_x,k_y)}{D_e D_m}\, dk_x dk_y \quad , \tag{2.31}$$

which, however, can be facilitated by changing to polar coordinates k,ϕ where

$$k_x = k\cos\phi \quad , \tag{2.32}$$

$$k_y = k\sin\phi \quad . \tag{2.33}$$

Thus,

$$r = \int_{C_k} k\,dk \int_0^{2\pi} \frac{F(k,\phi)}{D_e D_m}\, d\phi \quad . \tag{2.34}$$

The contour C_k for the k integration is shown in Figure 2.2. The branch cuts for the branch points $k = \pm k_o$ are defined by the analytic properties that

a) $\text{Im } k_{z2} = \text{Im } \sqrt{k_o^2 - k^2} < 0$ on the entire top Riemann sheet;

b) $\text{Re } k_{z2} > 0$ in the first and third quadrants; and

c) $\text{Re } k_{z2} < 0$ in the second and fourth quadrants.

However, $k = \pm \sqrt{\varepsilon_r}\, k_o$ are not branch points since the integrand is a single-valued function of $k_{z1} = \sqrt{\varepsilon_r k_o^2 - k^2}$. The branch cuts are also shown in Figure 2.2.

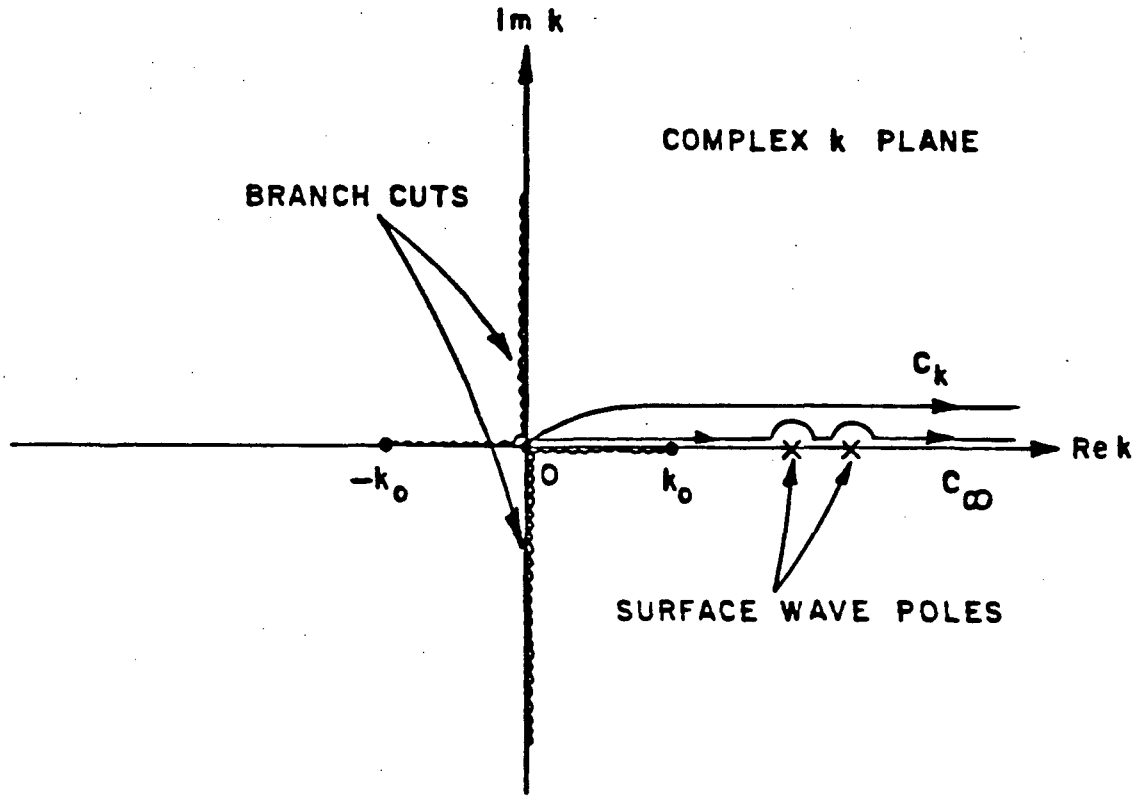

Figure 2.2. Proper contours of integration and branch cuts in the complex k plane.

The denominator in the integrand of Equation (2.24) defines the surface wave modes. These modes are determined by the roots of

$$D_e = 0 \quad \text{(for the TE waves)} \quad , \tag{2.35}$$

$$D_m = 0 \quad \text{(for the TM waves)} \quad . \tag{2.36}$$

Substituting $a = k_o t\sqrt{\varepsilon_r - 1}$ and $\sigma = t\sqrt{\varepsilon_r k_o^2 - k^2}$ into Equations (2.35) and (2.36) and rearranging terms yields, respectively,

$$\sqrt{a^2-\sigma^2} + \sigma\cot\sigma = 0 \quad , \tag{2.37}$$

$$-\varepsilon_r\sqrt{a^2-\sigma^2} + \sigma\tan\sigma = 0 \quad . \tag{2.38}$$

It can be demonstrated that if ε_r is real and $\varepsilon_r \neq 1$, the roots of Equations (2.37) and (2.38) are real and located inside the segment $k_o < k < \sqrt{\varepsilon_r}k_o$. If N_e, N_m represents the number of roots for the TE, TM case, respectively, then it can be shown that

$$N_e = \begin{cases} 0 & , \text{ for } a < \pi/2 \\ n & , \text{ for } (n-1/2)\pi < a < (n+1/2)\pi, \quad n = 1,2,3,\ldots \end{cases} ,$$

and

$$N_m = n+1 \quad , \text{ for } n\pi < a < (n+1)\pi, \; n = 0,1,2,\ldots \quad .$$

It is noted that the dominant TM mode has a zero cutoff frequency. For lossy dielectric (Im $\varepsilon_r \neq 0$), the roots just move off the real k-axis with the form $k = k_r - jk_i$, $k_i > 0$. The exact root locations can be determined by using the Newton-Rhapson procedure.

For efficient numerical evaluation of the integral in Equation (2.34), the new contour C_∞ is adopted by deforming C_k (as shown in Figure 2.2). The integration along C_∞ is performed by computing the Cauchy value of the integrals around the surface wave poles. Assuming the surface wave poles constitute an ordered set as $\{p_\ell,\ \ell=1,2,\ldots,n\}$, Equation (2.34) can be written as

$$\Gamma = \lim_{\delta\to 0^+} \left[\int_0^{p_1-\delta} + \int_{p_1+\delta}^{p_2-\delta} + \cdots + \int_{p_{n-1}+\delta}^{p_n-\delta} + \int_{p_n+\delta}^{\infty} \right] k\,dk \int_0^{2\pi} \frac{F(k,\phi)}{D_e D_m}\, d\phi$$

$$- j\pi \sum_{\ell=1}^{n} \int_0^{2\pi} d\phi\ \text{Residue} \left[\frac{F(k,\phi)}{D_e D_m} \right]_{k=p_\ell} . \qquad (2.39)$$

In the case of lossy dielectric, the integrations from $p_\ell-\delta$ to $p_\ell+\delta$, $\ell=1,2,3,\ldots,n$, can be evaluated analytically without indenting the contour C_∞. This is done by using two terms of a Taylor series expansion of $D_e D_m$ about p_ℓ, and by taking the value of the numerator $F(k,\phi)$ at $k=p_\ell$ throughout the interval.

In actual numerical evaluation of (2-39), it is found [6] that $\delta \sim 0.001k_0$ is adequate, and the infinite integral should be terminated at k no less than 150 k_0 for the self impedance calculation. For the mutual

impedance calculation, however, this infinite integral tends to converge more slowly as the separation between the two dipole modes becomes larger, and hence will involve an exhorbitant amount of computer time. Special treatment is required to improve the computational efficiency, which is dealt with in the next chapter.

C. MUTUAL COUPLING ANALYSIS

In order to employ the method to analyze the mutual coupling between microstrip patch antennas, one needs to evaluate the elements of the impedance matrix and the voltage vector. Assuming the Galerkin form of the moment method is chosen, and the basis and weighting functions (modes) are members of the set $\{\bar{J}_m = \hat{x}J_{mx} + \hat{y}J_{my}: \quad m=1,2, \ldots, N < \infty\}$, the mutual impedance between mode J_m and mode J_n is defined as

$$z_{mn} = -\int_{Sn} \bar{E}_m(\bar{r}) \cdot \bar{J}_n(\bar{r}')d_s' \quad , \tag{2.40}$$

and the element of the voltage vector is defined as

$$v_m = \int_v \bar{E}_m(\bar{r}) \cdot \bar{J}_i(\bar{r}')d_v' \quad , \tag{2.41}$$

where $\bar{E}_m$ is the electric field excited by mode m, and $\bar{J}_i$ is the impressed current source. As presented in Appendix B, the exact expressions for z_{mn} and v_m are given by

$$z_{mn} = -\frac{j}{4\pi^2}\int\int_{-\infty}^{\infty}\left[\left[\left(k_y\tilde{\psi}_{e2} + \frac{k_x k_{z2}}{\omega\varepsilon_o}\tilde{\psi}_{m2}\right)\cos\phi_{mn}\right.\right.$$

$$\left.\left. - \left(k_x\tilde{\psi}_{e2} - \frac{k_y k_{z2}}{\omega\varepsilon_o}\tilde{\psi}_{m2}\right)\sin\phi_{mn}\right]\tilde{J}_{nx}\right.$$

$$\left. - \left[\left(k_y\tilde{\psi}_{e2} + \frac{k_x k_{z2}}{\omega\varepsilon_o}\tilde{\psi}_{m2}\right)\sin\phi_{mn} + \left(k_x\tilde{\psi}_{e2} - \frac{k_y k_{z2}}{\omega\varepsilon_o}\tilde{\psi}_{m2}\right)\cos\phi_{mn}\right]\tilde{J}_{ny}\right]$$

$$\cdot\, e^{-j(k_x x_{mn} + k_y y_{mn})}\, dk_x dk_y \quad , \tag{2.42}$$

$$v_m = -\frac{jI_i}{4\pi^2}\int\int_{-\infty}^{\infty}\frac{(k_x^2+k_y^2)}{\omega\varepsilon_o\varepsilon_r k_{z1}}\tilde{\psi}_{m1}e^{-j(k_x x_f + k_y y_f)}\sin k_{z1}t\, dk_x dk_y \quad , \tag{2.43}$$

where

$$\tilde{\psi}_{m1} = -\frac{j\varepsilon_r k_{z2}}{(k_x^2+k_y^2)D_m}\left(k_x\tilde{J}_{mx} + k_y\tilde{J}_{my}\right) \quad , \tag{2.44}$$

$$\tilde{\psi}_{e2} = \frac{\omega\mu_o \sin k_{z1}t}{(k_x^2+k_y^2)D_e}\left(k_x\tilde{J}_{my} - k_y\tilde{J}_{mx}\right) \quad , \tag{2.45}$$

$$\tilde{\psi}_{m2} = -\frac{k_{z1}\sin k_{z1}t}{(k_x^2+k_y^2)D_m}\left(k_x\tilde{J}_{mx} + k_y\tilde{J}_{my}\right) \quad , \tag{2.46}$$

$$\mathcal{J}_{mx} = \int_{-y_m}^{y_m} \int_{-x_m}^{x_m} J_{mx}(x,y) e^{j(k_x x + k_y y)} \, dxdy \quad , \tag{2.47}$$

$$\mathcal{J}_{my} = \int_{-y_m}^{y_m} \int_{-x_m}^{x_m} J_{my}(x,y) e^{j(k_x x + k_y y)} \, dxdy \quad , \tag{2.48}$$

$$\tilde{J}_{nx'} = \int_{-y_n}^{y_n} \int_{-x_n}^{x_n} J_{nx'}(x',y') \, e^{-j[x'(k_x \cos\phi_{mn} + k_y \sin\phi_{mn}) + y'(-k_x \sin\phi_{mn} + k_y \cos\phi_{mn})]} dx'dy' \quad , \tag{2.49}$$

$$\tilde{J}_{ny'} = \int_{-y_n}^{y_n} \int_{-x_n}^{x_n} J_{ny'}(x',y') \, e^{-j[x'(k_x \cos\phi_{mn} + k_y \sin\phi_{mn}) + y'(-k_x \sin\phi_{mn} + k_y \cos\phi_{mn})]} dx'dy' \quad , \tag{2.50}$$

ϕ_{mn} is the angle between the x-axis of mode m and the x'-axis of mode n; $2x_m$ and $2y_m$ are the widths of mode m on in the x and y directions, respectively, and likewise, $2x_n$, $2y_n$ are the widths of mode n in the x',y' directions (see Figure 2.3). Also, (x_f,y_f) denotes the coordinates of the feed location with respect to the (x,y) axis centered on mode m.

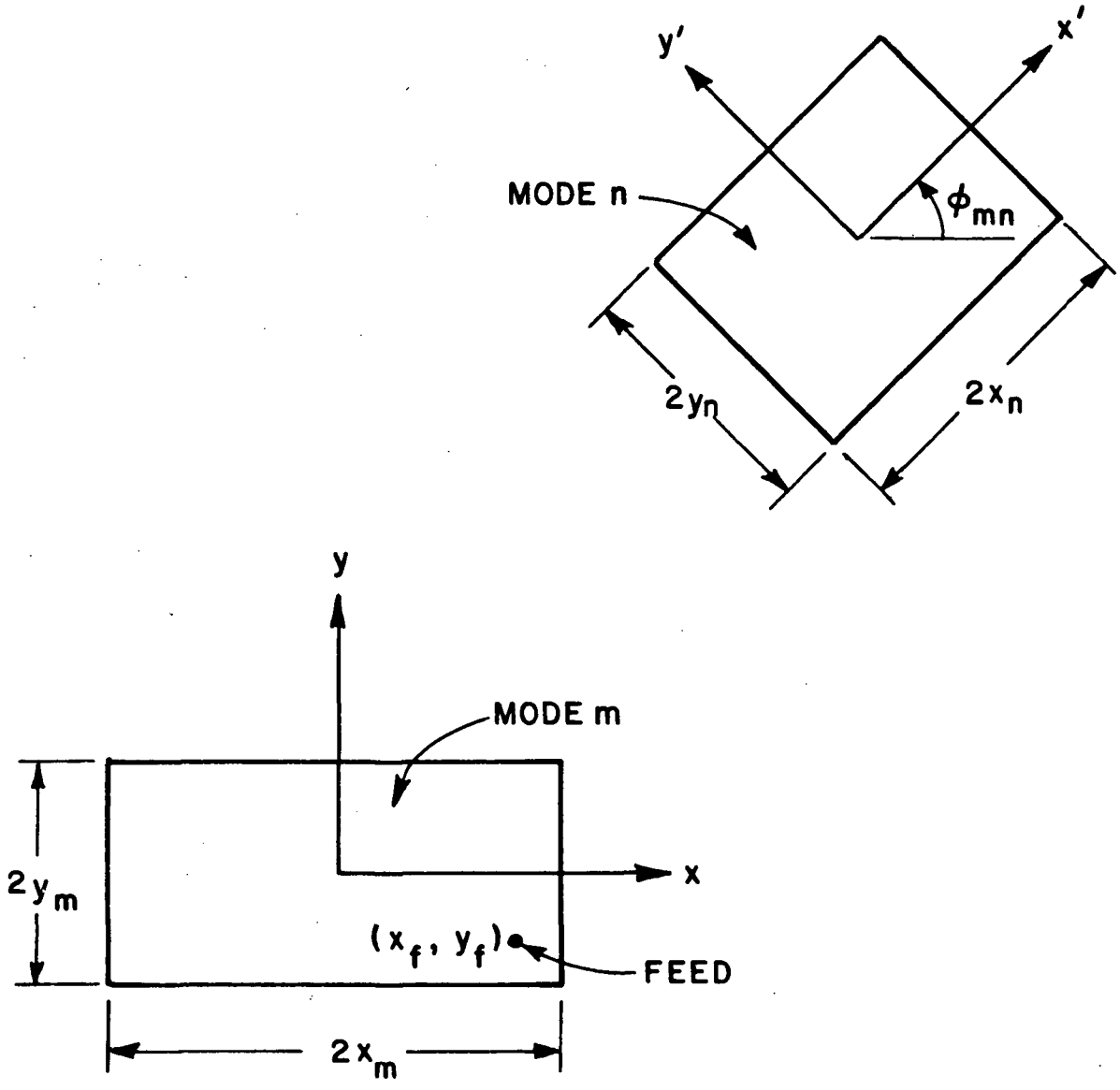

Figure 2.3. Geometry of patch dipoles m and n.

As $k = \sqrt{k_x^2 + k_y^2} \to \infty$, the integrands in Equations (2.42) and (2.43) become highly oscillatory. This will cause numerical difficulty in evaluating z_{mn} and v_m accurately. To rectify the situation, it is important to note the asymptotic behavior of these integrands as k tends to infinity. Defining

$$T_1 = k_y \tilde{\psi}_{e2} + \frac{k_x k_{z2}}{\omega\varepsilon_o} \tilde{\psi}_{m2}$$

$$= \frac{1}{\omega\varepsilon_o} \left\{ \frac{k_o^2 k_y}{D_e} \left[k_x \tilde{J}_{my} - k_y \tilde{J}_{mx} \right] - \frac{k_x k_{z1} k_{z2}}{D_m} \left[k_x \tilde{J}_{mx} - k_y \tilde{J}_{my} \right] \right\} \frac{\sin k_{z1} t}{(k_x^2 + k_y^2)}, \tag{2.51}$$

and

$$T_2 = k_x \tilde{\psi}_{e2} - \frac{k_y k_{z2}}{\omega\varepsilon_o} \tilde{\psi}_{m2}$$

$$= \frac{1}{\omega\varepsilon_o} \left\{ \frac{k_o^2 k_x}{D_e} \left[k_x \tilde{J}_{my} - k_y \tilde{J}_{mx} \right] + \frac{k_y k_{z1} k_{z2}}{D_m} \left[k_x \tilde{J}_{mx} + k_y \tilde{J}_{my} \right] \right\} \frac{\sin k_{z1} t}{(k_x^2 + k_y^2)}, \tag{2.52}$$

one can rewrite Z_{mn} as

$$Z_{mn} = \frac{-j}{4\pi^2} \int_{-\infty}^{\infty} \int \{ T_1 [\tilde{J}_{nx}, \cos\phi_{mn} - \tilde{J}_{ny}, \sin\phi_{mn}] - T_2 [\tilde{J}_{nx}, \sin\phi_{mn} + \tilde{J}_{ny}, \cos\phi_{mn}] \} e^{-j(k_x x_{mn} + k_y y_{mn})} dk_x dk_y \quad . \tag{2.53}$$

Noting that $k_{z1}, k_{z2} \to -jk$, $\sin k_{z1}t \to \frac{e^{kt}}{j^2}$ and $\cos k_{z1}t \to \frac{e^{kt}}{2}$ as $k \to \infty$, one can approximate, for large k,

$$D_e \simeq -jke^{kt} \quad , \tag{2.54}$$

$$D_m \simeq -jk \frac{(\varepsilon_r+1)}{2} e^{kt} \quad , \tag{2.55}$$

and hence,

$$T_1 \simeq -\frac{\eta_o}{2k_o} \frac{1}{\frac{k(\varepsilon_r+1)}{2}} \left\{ \left[k_o^2 \frac{(\varepsilon_r+1)}{2} - k_x^2 \right] \tilde{J}_{mx} - k_x k_y \tilde{J}_{my} \right\} \quad , \tag{2.56}$$

$$T_2 \simeq +\frac{\eta_o}{2k_o} \frac{1}{\frac{k(\varepsilon_r+1)}{2}} \left\{ \left[k_o^2 \frac{(\varepsilon_r+1)}{2} - k_y^2 \right] \tilde{J}_{my} - k_x k_y \tilde{J}_{mx} \right. \quad , \tag{2.57}$$

Similarly,

$$v_m = \frac{-jI_i}{4\pi^2} \int\int_{-\infty}^{\infty} T_3 \, e^{-j(k_x x_f + k_y y_f)} \, dk_x d_{ky} \quad , \tag{2.58}$$

where

$$T_3 = -\frac{j}{\omega\varepsilon_o} \frac{\sin k_z t}{D_m} (k_x \tilde{J}_{mx} + k_y \tilde{J}_{my}) \quad , \tag{2.59}$$

and, for large k,

$$T_3 \simeq -\frac{j\eta_o}{2k_o} \frac{1}{\frac{k(\varepsilon_r+1)}{2}} (k_x \tilde{J}_{mx} + k_y \tilde{J}_{my}) \quad . \tag{2.60}$$

The asymptotic forms of T_1, T_2 and T_3 will be utilized in the next chapter to improve the computational efficiency of z_{mn} and v_m.

Finally, the proper choice of the dipole modes $\tilde{J}_m$, m=1,2,...,N, and their corresponding transforms are discussed in Appendix C.

III. IMPROVING THE COMPUTATIONAL EFFICIENCY

A. INTRODUCTION

As mentioned in the last chapter, the integrals for z_{mn} or v_m converge slowly (especially for large separation between two dipole modes, or a dipole mode and the impressed source) when $k \to \infty$. Moreover, as k becomes large, the corresponding integrand will get highly oscillatory, and will require very small step size in the numerical integration scheme. All these translate into large amounts of computer-time, and hence high costs. It is, therefore, of great interest to improve the computational efficiency of z_{mn} or v_m. As suggested by Pozar [6], it is useful to construct an integral that have two different representations such that the first can be evaluated easily, while the second will have the identical asymptotic behavior as that of z_{mn} or v_m. It is then reasonable to expect the integral for the difference of z_{mn} or v_m and the constructed integral to converge much faster because of their identical asymptotic forms. The total value of z_{mn} or v_m can be recovered by adding back the constructed integral which is evaluated via its first representation. With such manipulation, the overall efficiency for calculating z_{mn} or v_m can be improved.

This chapter is devoted to the construction of such integrals. In particular, Section B will concentrate on the integral representations which exhibit asymptotic behavior identical to those of z_{mn} and v_m. The alternative representations (which can be evaluated easily) will be discussed in Section C.

B. MUTUAL COUPLING IN A GROUNDED HOMOGENEOUS MEDIUM

In this section, an analysis similar to that of Chapter 2 will be repeated for a homogeneous dielectric half space D bounded by a conducting plane, where μ_o and $\varepsilon_o\varepsilon_e$ are the constitutive parameters.

Consider a conducting patch S of current density $\bar{J}_s$ in the x-y plane situated at a distance t from the ground plane in D (Figure 3.1). The vector potential $\bar{A}$ due to $\bar{J}_s$ is given by

$$\bar{A}(\bar{r}) = \frac{1}{4\pi} \int_S \left[\frac{e^{-jk_e r_s}}{r_s} - \frac{e^{-jk_e r_i}}{r_i} \right] \bar{J}_s(\bar{r}')\, ds' \quad , \; z > -t \qquad (3.1)$$

where $k_e = w\sqrt{\mu_o \varepsilon_o \varepsilon_e}$,

$$\bar{r} = \hat{x}x + \hat{y}y + \hat{z}z \quad ,$$

$$\bar{r}' = \hat{x}x' + \hat{y}y' \quad ,$$

$$\bar{r}_s = \bar{r} - \bar{r}' = \hat{x}(x-x') + \hat{y}(y-y') + \hat{z}z \quad , \quad r_s = |\bar{r}_s| \quad ,$$

$$\bar{r}_i = \bar{r} - \bar{r}' + \hat{z}2t = \hat{x}(x-x') + \hat{y}(y-y') + \hat{z}(z+2t)$$

and,

$$\bar{J}_s(\bar{r}') = \hat{x}J_{sx}(\bar{r}'^{1}) + \hat{y}J_{sy}(\bar{r}^{1}) \quad .$$

Homogeneous dielectric half space D

$\mu_o, \varepsilon_o \varepsilon_e$

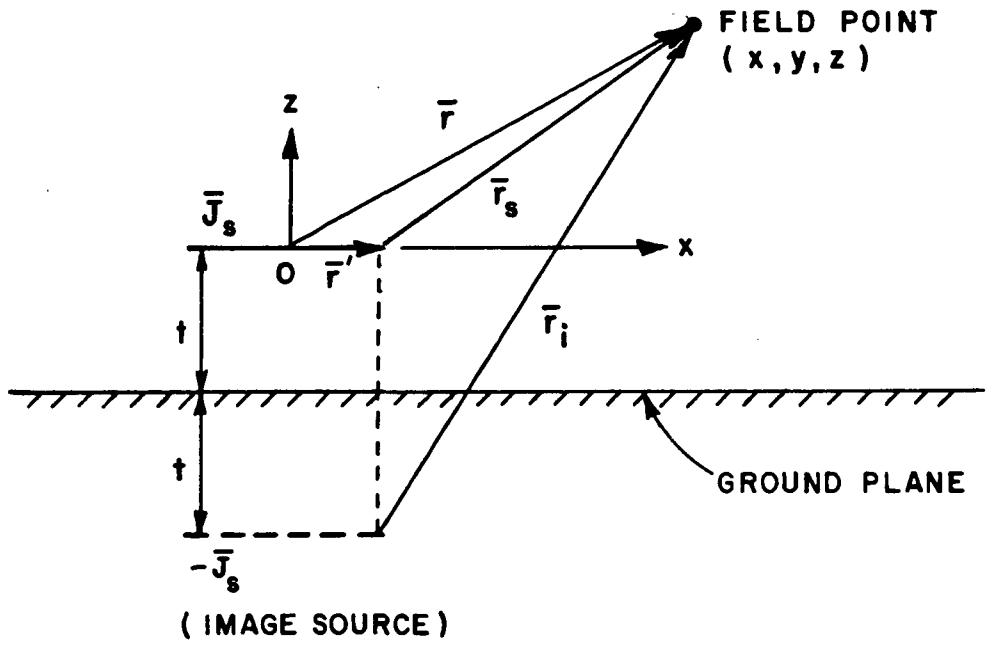

Figure 3.1. Patch current source $\bar{J}_s$ in homogeneous dielectric half space D.

Employing the identity

$$\frac{e^{-jk_e R}}{R} = \frac{1}{j2\pi} \int\int_{-\infty}^{\infty} \frac{1}{k_z} e^{-j[k_x(x-x') + k_y(y-y') + k_z|z-z'|]} dk_x dk_y , \tag{3.2}$$

where $R = |\bar{R}| = |\hat{x}(x-x') + \hat{y}(y-y') + \hat{z}(z-z')|$, and

$$k_z = \sqrt{k_e^2 - k_x^2 - k_y^2} \quad , \text{ with } \mathrm{Im} k_z < 0 \quad , \tag{3.3}$$

one can write

$$\bar{A}(\bar{r}) = \frac{1}{4\pi^2} \int\int\int_{S-\infty}^{\infty} \frac{\bar{J}_s(\bar{r}')}{j2k_z} \left[e^{-j\phi_s} - e^{-j\phi_i} \right] dk_x\, dk_y\, ds', \; z > -t, \tag{3.4}$$

where

$$\phi_s = \phi_s(\bar{r}, k_x, k_y) = k_x(x-x') + k_y(y-y') + k_z|z| \quad , \tag{3.5}$$

$$\phi_i = \phi_i(\bar{r}, k_x, k_y) = k_x(x-x') + k_y(y-y') + k_z(z+2t) \quad , \tag{3.6}$$

It is well-known that the electric field $\bar{E}$ at $\bar{r} \epsilon D$ is given by

$$\bar{E}(\bar{r}) = \frac{-j\eta_0}{k_0} \left[k_0^2 \bar{A}(\bar{r}) + \frac{1}{\epsilon_e} \nabla\nabla \cdot \bar{A}(\bar{r}) \right] \quad , \tag{3.7}$$

where $\eta_0 = \sqrt{\mu_0/\epsilon_0}$ and $k_0 = \omega\sqrt{\mu_0\epsilon_0}$.

Since

$$\nabla \cdot \bar{A}(\bar{r}) = \frac{\partial}{\partial x} A_x(\bar{r}) + \frac{\partial}{\partial y} A_y(\bar{r}) + \frac{\partial}{\partial z} A_z(\bar{r})$$

$$= \frac{1}{4\pi^2} \iiint_{S-\infty}^{\infty} \frac{1}{j2k_z} \left\{ -jk_x \left[e^{-j\phi_s} - e^{-j\phi_i} \right] J_{sx}(\bar{r}') - \right.$$

$$\left. -jk_y \left[e^{-j\phi_s} - e^{-j\phi_i} \right] J_{sy}(\bar{r}') \right\} dk_x dk_y ds' \qquad (3.8)$$

one will find

$$\nabla\nabla\cdot\bar{A}(\bar{r}) = \left[\hat{x} \frac{\partial}{\partial x} + \hat{y} \frac{\partial}{\partial y} + \hat{z} \frac{\partial}{\partial z} \right] \nabla\cdot\bar{A}(\bar{r}) \qquad (3.9)$$

$$= \frac{1}{4\pi^2} \iiint_{S-\infty}^{\infty} \frac{1}{j2k_z} \left\{ \hat{x} \left[-k_x^2 \left(e^{-j\phi_s} - e^{-j\phi_i} \right) J_{sx}(\bar{r}) - k_x k_y \right. \right.$$

$$\left. \left(e^{-j\phi_s} - e^{-j\phi_i} \right) J_{sy}(\bar{r}') + \right.$$

$$+ \hat{y} \left[-k_x k_y \left(e^{-j\phi_s} - e^{-j\phi_i} \right) J_{sx}(\bar{r}') - k_y^2 \left(e^{-j\phi_s} - e^{-j\phi_i} \right) J_{sy}(\bar{r}') \right] +$$

$$+ \hat{z} \left[-k_x k_z \left(\mathrm{sgn}(z)\, e^{-j\phi_s} - e^{-j\phi_i} \right) J_{sx}(\bar{r}') - k_y k_z \left(\mathrm{sgn}(z)\, e^{-j\phi_s} - \right. \right.$$

$$\left. \left. \left. e^{-j\phi_i} \right) J_{sy}(\bar{r}') \right] \right\} dk_x dk_y ds' \quad .$$

Next it follows from Equations (3.4), (3.9) and (3.7) that

$$\bar{E}(\bar{r}) = \frac{-j\eta_o}{k_o} \cdot \frac{1}{4\pi^2} \int\int\int_{S-\infty}^{\infty} \frac{1}{j2k_z\varepsilon_e} \left\{ \hat{x} \left(\left[\bar{\varepsilon_e k_o^2 - k_x^2} \right] J_{sx}(\bar{r}') - k_x k_y J_{sy}(\bar{r}') \right) \left(e^{-j\phi_s} - e^{-j\phi_i} \right) + \hat{y} \left(\left[\bar{\varepsilon_e k_o^2 - k_y^2} \right] J_{sy}(\bar{r}') - k_x k_y J_{sx}(\bar{r}') \right) \left(e^{-j\phi_s} - e^{-j\phi_i} \right) - \right.$$
$$\left. -\hat{z} \left(k_x k_z J_{sx}(\bar{r}') + k_y k_z J_{sy}(\bar{r}') \right) \left(\mathrm{sgn}(z)\, e^{-j\phi_s} - e^{-j\phi_i} \right) \right\}$$
$$dk_x dk_y ds' \quad . \qquad (3.10)$$

Now one can readily formulate the mutual impedance z_{mn}^d between dipole mode m and mode n as

$$z_{mn}^d = - \int_{S_n} \bar{E}_m (\bar{r}+\bar{r}') \cdot \bar{J}_n(\bar{r}')\, ds' \quad , \qquad (3.11)$$

where $\bar{E}_m$ denotes the electric field in D excited by mode m with current density $\bar{J}_m(\bar{r})$ $\varepsilon\{\bar{J}_\alpha(\bar{r}) = \hat{x}\, J_{\alpha x} + \hat{y} J_{\alpha y} : \alpha=1,2,\ldots,N$, which exists on the surface patch S_m. The definitions of $\bar{r}$ and $\bar{r}'$ are obvious from Figure 3.2. Observing that

$$\bar{E}_m(\bar{r}+\bar{r}') = \hat{x}E_{mx}(\bar{r}+\bar{r}') + \hat{y}E_{my}(\bar{r}+\bar{r}') + \hat{z}E_{mz}(\bar{r}+\bar{r}')$$

$$= \hat{x}' \left[E_{mx}(\bar{r}+\bar{r}') \cos\phi_{mn} + E_{my}(\bar{r}+\bar{r}') \sin\phi_{mn} \right] +$$

$$\hat{y}' \left[-E_{mx}(\bar{r}+\bar{r}') \sin\phi_{mn} + E_{my}(\bar{r}+\bar{r}') \cos\phi_{mn} \right] +$$

$$\hat{z}E_{mz}(\bar{r}+\bar{r}') \qquad (3.12)$$

and

$$\bar{J}_n(\bar{r}') = \hat{x}J_{nx'}(\bar{r}') + \hat{y}'J_{ny'}(\bar{r}') \quad , \qquad (3.13)$$

and making use of Equation (3.10), one can rewrite Equation (3.11) as

$$z_{mn}^d = \frac{j\eta_o}{4\pi^2 k_o} \int_{-\infty}^{\infty}\int \frac{1}{j2k_z\varepsilon_e} \left\{ \left[(\varepsilon_e k_o^2 - k_x^2)\, \tilde{J}_{mx} - k_x k_y\, \tilde{J}_{my} \right] \right.$$

$$\left[\tilde{J}_{nx'}\cos\phi_{mn} - \tilde{J}_{ny'}\sin\phi_{mn} \right] +$$

$$\left. + \left[(\varepsilon_e k_o^2 - k_y^2)\, \tilde{J}_{my} - k_x k_y \tilde{J}_{mx} \right] \left[\tilde{J}_{nx'}\sin\phi_{mn} + \tilde{J}_{ny'}\cos\phi_{mn} \right] \right\}$$

$$\left[e^{-j(k_x x_{mn} + k_y y_{mn})} \right] dk_x dk_y \quad , \qquad (3.14)$$

where $\tilde{J}_{mx}$, $\tilde{J}_{my}$, $\tilde{J}_{nx'}$ and $\tilde{J}_{ny'}$ are defined in Equations (2.47), (2.48), (2.49) and (2.50).

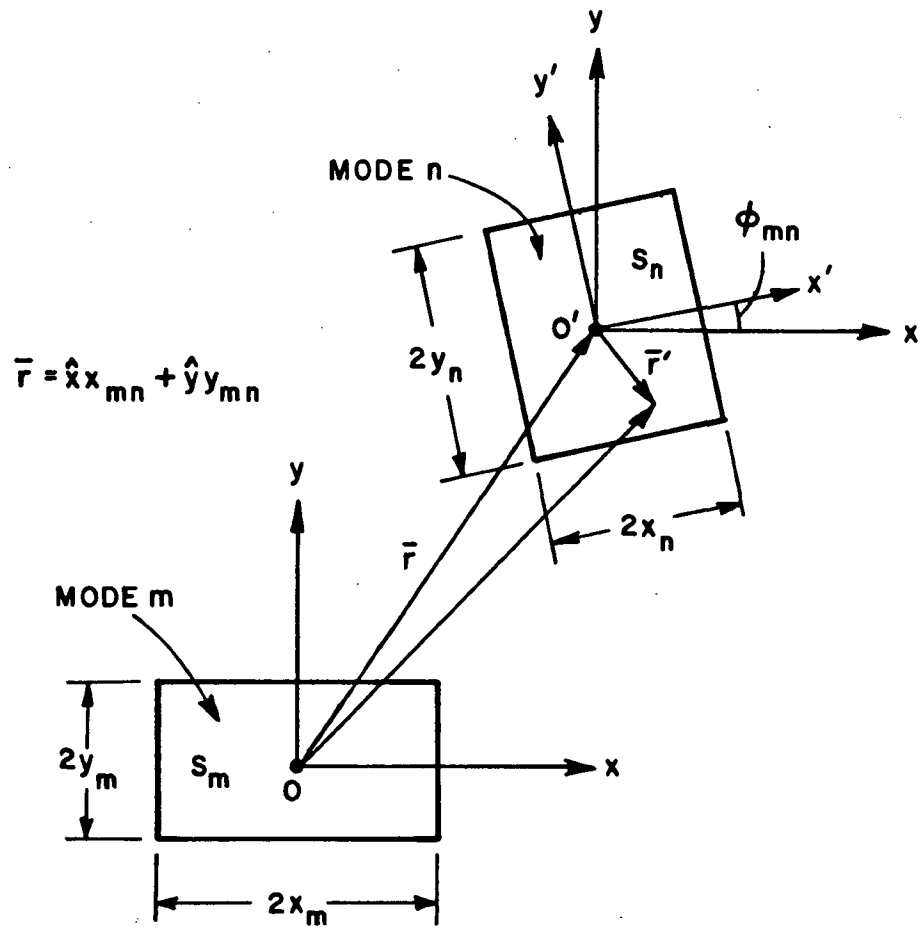

Figure 3.2. Configuration of dipole modes m and n in the z=0 plane.

Letting the impressed source $\bar{J}_i$ be a current filament of uniform amplitude I_i, normal to the ground plane, and situated at (x_f, y_f) with respect to the center of dipole mode m in the z=0 plane, i.e.,

$$\bar{J}_i(\bar{r}) = \hat{z} I_i \delta(x-x_f)\delta(y-y_f), \quad -t < z < 0 \quad , \tag{3.15}$$

the mutual impedance between mode m and the impressed source J_i can be written as

$$\begin{aligned} v_m^d &= \int_V \bar{E}_m(\bar{r}) \cdot \bar{J}_i(\bar{r}) dv \\ &= \int_{-t}^{0} I_i \, E_{mz}(x_f, y_f, z) \, d_z \\ &= \frac{-j\eta_0 I_i}{4\pi^2 k_0} \int\int_{-\infty}^{\infty} \frac{1}{j2k_z\varepsilon_e} \left\{ \left[k_x k_z \tilde{J}_{mx} + k_y k_z \tilde{J}_{my} \right] \right. \\ &\qquad \left. \left[e^{-j(k_x x_f + k_y y_f)} \right] \right. \\ &\qquad \int_{-t}^{0} \left[e^{jk_z z} + e^{-jk_z 2t - jk_z z} \right] dz dk_x dk_y \end{aligned}$$

or

$$v_m^d = \frac{j\eta_0 I_i}{4\pi^2 k_0} \int\int_{-\infty}^{\infty} \frac{1}{2k_z\varepsilon_e} \left[k_x \tilde{J}_{mx} + k_y \tilde{J}_{my} \right] \left[1 - e^{-j2k_z t} \right] e^{-j(k_x x_f + k_y y_f)} \, dk_x dk_y \quad . \tag{3.16}$$

In order to compare the asymptotic forms of the integrands of z_{mn}^d and v_m^d with those of z_{mn} and v_m in Chapter 2, it is convenient to express z_{mn}^d and v_m^d in the following forms:

$$z_{mn}^d = \frac{-j}{4\pi^2} \int_{-\infty}^{\infty}\int \left\{ T_1^d \left[\tilde{J}_{nx}, \cos\phi_{mn} - \tilde{J}_{ny}, \sin\phi_{mn} \right] - T_2^d \left[\tilde{J}_{nx}, \sin\phi_{mn} + \tilde{J}_{ny}, \cos\phi_{mn} \right] \right\} e^{-j(k_x x_{mn} + k_y y_{mn})} \, dk_x dk_y \quad , \tag{3.17}$$

$$v_m^d = \frac{-jI_i}{4\pi^2} \int_{-\infty}^{\infty}\int T_3^d \, e^{-j(k_x x_f + k_y y_f)} \, dk_x d_{ky} \quad , \tag{3.18}$$

where

$$T_1^d = \frac{-\eta_o}{j^2 k_o k_z \varepsilon_e} \left[(\varepsilon_e k_o^2 - k_x^2) \, \tilde{J}_{mx} - k_x k_y \tilde{J}_{my} \right] \quad , \tag{3.19}$$

$$T_2^d = \frac{\eta_o}{j^2 k_o k_z \varepsilon_e} \left[(\varepsilon_e k_o^2 - k_y^2) \, \tilde{J}_{my} - k_x k_y \tilde{J}_{mx} \right] \quad , \tag{3.20}$$

and

$$T_3^d = \frac{-\eta_o}{2 k_o k_z \varepsilon_e} \left(k_x \tilde{J}_{mx} + k_y \tilde{J}_{my} \right) \left(1 - e^{-j2k_z t} \right) \quad . \tag{3.21}$$

As $k = \sqrt{k_x^2 + k_y^2} \to \infty$, $k_z \to -jk$, and thus one can write, for large k,

$$T_1^d \simeq \frac{-\eta_o}{2k_o k\varepsilon_e} \left[(\varepsilon_e k_o^2 - k_x^2)\, \tilde{J}_{mx} - k_x k_y\, \tilde{J}_{my} \right] , \tag{3.22}$$

$$T_2^d \simeq \frac{\eta_o}{2k_o k\varepsilon_e} \left[(\varepsilon_e k_o^2 - k_y^2)\, \tilde{J}_{my} - k_x k_y\, \tilde{J}_{mx} \right] , \tag{3.23}$$

and

$$T_3^d \simeq \frac{-j\eta_o}{2k_o k\varepsilon_e} \left(k_x\, \tilde{J}_{mx} + k_y\, \tilde{J}_{my} \right) . \tag{3.24}$$

Comparing Equations (2.51), (2.52) and (2.53) with Equations (3.22), (3.23) and (3.24), it is readily seen that choosing

$$\varepsilon_e = \frac{(\varepsilon r+1)}{2} \tag{3.25}$$

will make $T_\alpha \equiv T_\alpha^d$, $\alpha=1,2,3$, for large k. In other words, if one considers the grounded, homogeneous, dielectric half space D with ε_e specified by Equation (3.25), then the following integrals:

$$\Gamma_{mn} = z_{mn} - z_{mn}^d \tag{3.26}$$

$$= \frac{-j}{4\pi^2} \int_{-\infty}^{\infty}\int \left\{ (T_1 - T_1^d) \left[\tilde{J}_{nx}, \cos\phi_{mn} - \tilde{J}_{my}, \sin\phi_{mn} \right] - \right.$$

$$\left. - (T_2 - T_2^d) \left[\tilde{J}_{nx}, \sin\phi_{mn} + \tilde{J}_{ny}, \cos\phi_{mn} \right] \right\} e^{-j(k_x x_{mn} + k_y y_{mn})}\, dk_x dk_y$$

and

$$P_m = v_m - v_m^d \tag{3.27}$$

$$= \frac{-jI_i}{4\pi^2} \int_{-\infty}^{\infty}\int \begin{bmatrix} & \\ T_3 - T_3^d & \end{bmatrix} e^{-j(k_x x_f + k_y y_f)}\, dk_x dk_y \quad ,$$

will converge rapidly since the functions $(T_\alpha - T_\alpha^d)$, $\alpha=1,2,3$, vanish identically for large k. One can compute Γ_{mn} and P_m according to Equations (3.26) and (3.27), and z_{mn}^d and v_m^d via the alternative forms to be discussed in the next section, whereby z_{mn} and v_m can be evaluated efficiently as

$$Z_{mn} = \Gamma_{mn} + Z_{mn}^d \quad , \tag{3.28}$$

and

$$v_m = P_m + v_m^d \quad . \tag{3.29}$$

C. ALTERNATIVE FORMS OF z_{mn}^d and v_m^d

In this section, expressions of z_{mn}^d and v_m^d are obtained directly from the vector potential that employs the homogeneous space Green's function instead of its plane wave expansion. Thereby the resulting expressions are easier to compute, especially when the two dipole modes, or the dipole mode and the impressed source are well separated and t is not too small.

Referring to Figure 3.2, the vector potential $\bar{A}_m$ due to dipole mode m can be written in terms of the Green's function of the homogeneous half space D as follows:

$$\bar{A}_m(\bar{r}+\bar{r}') = \frac{1}{4\pi} \int_{Sm} \left[\frac{e^{-jk_e R_{mns}}}{R_{mns}} - \frac{e^{-jk_e R_{mni}}}{R_{mni}} \right] \bar{J}_m(x,y)\, dxdy, \quad (3.30)$$

for $\bar{r} = \hat{x}x_{mn} + \hat{y}y_{mn}$, and $\bar{r}' \epsilon S_n$, where

$$R_{mns} = |\bar{R}_{mns}|$$

$$= |\hat{x}(x_{mn} + x'\cos\phi_{mn} - y'\sin\phi_{mn} - x) +$$

$$+ \hat{y}(y_{mn} + x'\sin\phi_{mn} + y'\cos\phi_{mn} - y)|$$

and

$$R_{mni} = |\bar{R}_{mni}|$$

$$= |\bar{R}_{mns} + \hat{z}2t| \quad .$$

Making use of Equation (3.7), it can be shown (by direct calculation) that the electric field at $\bar{r}+\bar{r}'$ due to mode m is given by

$$\bar{E}_m(\bar{r}+\bar{r}') = \frac{j\eta_e}{4\pi k_e} \int_{Sm} dxdy \left\{ (\bar{J}_m(x,y)Q_1(\bar{R}_{mns}) + (\bar{J}_m(x,y) \cdot \hat{R}_{mns})\hat{R}_{ms}Q_2(\bar{R}_{mns})) \right.$$

$$- (\bar{J}_m(x,y)Q_1(\bar{R}_{mni}) + (\bar{J}_m(x,y)\cdot\hat{R}_{mni})\hat{R}_{mni}Q_2(\bar{R}m_{ni}))\Big\} \quad , \qquad (3.31)$$

where $Q_1(\bar{R}) = (1+jk_eR-k_e^2R^2)\ e^{-jk_eR}/R^3$, (3.32)

$$Q_2(\bar{R}) = (3+j3k_eR-k_e^2R^2)\ e^{-jk_eR}/R^3 \quad , \qquad (3.33)$$

$R = |\bar{R}|$, $\hat{R}$ is the unit vector in the direction of $\bar{R}$,

$k_e = \omega\sqrt{\mu_o\varepsilon_o\varepsilon_e}$ and $\eta_e = \sqrt{\mu_o/\varepsilon_o\varepsilon_e}$

From the definitions of z_{mn}^d and v_m^d, it is seen that

$$z_{mn}^d = -\int_{S_n} dx'dy'\bar{J}n(x',y') \cdot \left[\frac{j\eta_e}{4\pi k_e}\int_{Sm} dxdy\ \{(\bar{J}_m(x,y)Q_1(\bar{R}_{mns}) +\right.$$

$$+ (\bar{J}_m(x,y)\cdot\hat{R}_{mns})\ \hat{R}_{mns}Q_2(\bar{R}_{mns})) - (\bar{J}_m(x,y)Q_1(\bar{R}_{mni}) +$$

$$\left. + (\bar{J}_m(x,y)\cdot\hat{R}_{mni})\ \hat{R}_{mni}\ Q_2(\bar{R}_{mni}))\}\right] \quad , \qquad (3.34)$$

and

$$v_m^d = \int_{-t}^{o} dz\bar{J}_i(x_f,y_f,z) \cdot \left[\frac{j\eta_e}{4\pi k_e}\int_{S_m} dxdy\ \{(\bar{J}_m(x,y)Q_1(\bar{R}_fs) +\right.$$

$$\left. + (\bar{J}_m(x,y)\cdot\hat{R}_{fs})\ \hat{R}_{fs}Q_2(\bar{R}_{fs})) - (\bar{J}_m(x,y)Q_1(\bar{R}_{fi}) +\right.$$

$$+ \left(\bar{J}_m(x,y) \cdot \hat{R}_{fi}\right) \hat{R}_{fi} Q_2(\bar{R}_{fi})\Big\} \Big]_{-} \quad , \qquad (3.35)$$

where $\bar{J}_i(x_f,y_f,z)$ is defined in Equation (3.15),

$$\bar{R}_{fs} = \hat{x}(x_f-x) + \hat{y}(y_f-y) + \hat{z}z \quad , \quad R_{fs} = |\bar{R}_{fs}| \quad ,$$

and

$$\bar{R}_{fi} = \hat{x}(x_f-x) + \hat{y}(y_f-y) + \hat{z}(z+2t) \quad , \quad R_{fi} = |\bar{R}_{fi}| \quad .$$

It may be remarked that in computing z^d_{mn} and v^d_m using Equations (3.34) and (3.35) one will encounter some numerical difficulty (namely, the loss of accuracy due to the differencing of two terms of almost equal values) when t is small. In such case, it is appropriate to expand the Q_1 and Q_2 functions as Taylor series, and to keep the first few leading terms. Expansions about z=-t may be most adequate.

IV. SUMMARY

This report has presented expressions for:

1. the self or mutual impedance between microstrip expansion and test modes

2. the mutual impedance between a microstrip mode and a vertical current filament in the dielectric.

These are the main quantities needed in an MM solution of the microstrip antenna. Methods for the efficient evaluation of the impedances are presented. Finally, expansion modes are described which would be useful in analyzing the microstrip antenna over a wide frequency band.

REFERENCES

[1] D. M. Pozar, "Impedance and Mutual Coupling of Rectangular Microstrip Antennas", IEEE Trans. on Antennas and Propagation, Vol. AP-30, November 1982, pp. 1191-1196.

[2] E. H. Neuman, J. H. Richmond, and B. W. Kwan, "Mutual IMpedance Computation Between Microstrip Antennas", IEEE Trans. on Microwave Theory and Techniques, Vol. MTT-31, November 1983, pp. 941-945.

[3] M. D. Deshpande and M. C. Bailey, "Input Impedance of Microstrip Antennas", IEEE Trans. on Antennas and Propagation, Vol. AP-30, July 1982, pp. 645-650.

[4] M. C. Bailey and M. D. Deshpande, "Integral Equation Formulation of Microstrip Antennas", IEEE Trans. on Antennas and Propagation, Vol. AP-30, July 1982, pp. 651-656.

[5] E. H. Newman and P. Tulyathn, "Analysis of Microstrip Antennas Using Moment Methods", IEEE Trans. on Antennas and Propagation, Vol. AP-29, January 1981, pp. 47-53.

[6] D. M. Pozar, "Improved Computational Efficiency for the Moment Method Solution of Printed Dipoles and Patches", Electromagnetics, Vol. 3, July-December 1983, pp. 299-310.

[7] R. F. Harrington, Time Harmonic Electromagnetic Fields, McGraw-Hill, New York, 1961.

APPENDIX A

DETERMINATION OF SPECTRAL FUNCTIONS

Expanding Equations (2.2) and (2.3) in rectangular coordinates and making use of (2.4) and (2.5) yields the following:

In region 1 (dielectric),

$$E_{x1}(\bar{r}) = -\frac{\partial}{\partial y}\psi_{e1} + \frac{1}{j\omega\varepsilon_1}\frac{\partial^2}{\partial x \partial z}\psi_{m1}$$

$$= \frac{j}{4\pi^2}\iint_{-\infty}^{\infty}\left\{k_y\tilde{\psi}_{e1} - \frac{j}{\omega\varepsilon_1}k_x k_{z1}\tilde{\psi}_{m1}\right\} e^{-j(k_x x + k_y y)} \sin k_{z1}(z+t)\,dk_x dk_y \,, \tag{A.1}$$

$$E_{y1}(\bar{r}) = \frac{\partial}{\partial x}\psi_{e1} + \frac{1}{j\omega\varepsilon_1}\frac{\partial^2}{\partial y \partial x}\psi_{m1}$$

$$= \frac{-j}{4\pi^2}\iint_{-\infty}^{\infty}\left\{k_x\tilde{\psi}_{e1} + \frac{j}{\omega\varepsilon_1}k_y k_{z1}\tilde{\psi}_{m1}\right\} e^{-j(k_x x + k_y y)} \sin k_{z1}(z+t)\,dk_x dk_y \,, \tag{A.2}$$

$$E_{z1}(\bar{r}) = \frac{1}{j\omega\varepsilon_1}\left[\frac{\partial^2}{\partial z^2} + \varepsilon_r k_o^2\right]\psi_{m1}$$

$$= \frac{-j}{4\pi^2}\int\int_{-\infty}^{\infty} \frac{[k_x^2 + k_y^2]}{\omega\varepsilon_1}\ \tilde{\psi}_{m1}\ e^{-j(k_x x + k_y y)}\ \cos k_{z1}(z+t)\,dk_x dk_y\ ,$$

(A.3)

$$H_{x1}(\bar{r}) = \frac{1}{j\omega\mu_o}\frac{\partial^2}{\partial x \partial z}\psi_{e1} + \frac{\partial}{\partial y}\psi_{m1}$$

$$= \frac{j}{4\pi^2}\int\int_{-\infty}^{\infty}\left[\frac{jk_x\ k_{z1}}{\omega\mu_o}\ \tilde{\psi}_{e1} - k_y\tilde{\psi}_{m1}\right]\cos k_{z1}(z+t)e^{-j(k_x x + k_y y)}\,dk_x dk_y\ ,$$

(A.4)

$$H_{y1}(\bar{r}) = \frac{1}{j\omega\mu_o}\frac{\partial^2}{\partial y \partial z}\psi_{e1} - \frac{\partial}{\partial x}\psi_{m1}$$

$$= \frac{+j}{4\pi^2}\int\int_{-\infty}^{\infty}\left[\frac{jk_y\ k_{z1}}{\omega\mu_o}\ \tilde{\psi}_{e1} + k_x\tilde{\psi}_{m1}\right]e^{-j(k_x x + k_y y)}\cos k_{z1}(z+t)\,dk_x dk_y\ ,$$

(A.5)

$$H_{z1}(\bar{r}) = \frac{1}{j\omega\mu_0}\left(\frac{\partial^2}{\partial z^2} + \varepsilon_r k_o^2\right)\psi_{e1}$$

$$= \frac{-j}{4\pi^2}\int\int_{-\infty}^{\infty}\frac{1}{\omega\mu_0}(k_x^2 + k_y^2)\ \tilde{\psi}_{e1}\ e^{-j(k_x x + k_y y)}\ \sin k_{z1}(z+t)\,dk_x dk_y\ .$$

(A.6)

In region 2 (air),

$$E_{x2}(\bar{r}) = -\frac{\partial}{\partial y}\psi_{e2} + \frac{1}{j\omega\varepsilon_2}\frac{\partial^2}{\partial x \partial z}\psi_{m2}$$

$$= \frac{j}{4\pi^2}\int_{-\infty}^{\infty}\int\left\{k_y\tilde{\psi}_{e2} + \frac{k_x k_{z2}}{\omega\varepsilon_2}\tilde{\psi}_{m2}\right\} e^{-j(k_x x + k_y y + k_{z2} z)}\, dk_x dk_y \,, \tag{A.7}$$

$$E_{y2}(\bar{r}) = \frac{\partial}{\partial x}\psi_{e2} + \frac{1}{j\omega\varepsilon_2}\frac{\partial^2}{\partial y \partial z}\psi_{m2}$$

$$= \frac{-j}{4\pi^2}\int_{-\infty}^{\infty}\int\left\{k_x\tilde{\psi}_{e2} - \frac{k_y k_{z2}}{\omega\varepsilon_2}\tilde{\psi}_{m2}\right\} e^{-j(k_x x + k_y y + k_{z2} z)}\, dk_x dk_y \,, \tag{A.8}$$

$$E_{z2}(\bar{r}) = \frac{1}{j\omega\varepsilon_2}\left(\frac{\partial^2}{\partial z^2} + k_o^2\right)\psi_{m2}$$

$$= \frac{-j}{4\pi^2}\int_{-\infty}^{\infty}\int\frac{(k_x^2 + k_y^2)}{\omega\varepsilon_2}\tilde{\psi}_{m2}\, e^{-j(k_x x + k_y y + k_{z2} z)}\, dk_x dk_y \,, \tag{A.9}$$

$$H_{x2}(\bar{r}) = \frac{1}{j\omega\mu_o}\frac{\partial^2}{\partial x \partial z}\psi_{e2} + \frac{\partial}{\partial y}\psi_{m2}$$

$$= \frac{j}{4\pi^2}\int_{-\infty}^{\infty}\int\left[\frac{k_x\, k_{z2}}{\omega\mu_o}\tilde{\psi}_{e2} - k_y\tilde{\psi}_{m2}\right] e^{-j(k_x x + k_y y + k_{z2} z)}\, dk_x dk_y \,, \tag{A.10}$$

$$H_{y2}(\bar{r}) = \frac{1}{j\omega\mu_0} \frac{\partial^2}{\partial y \partial z} \psi_{e2} - \frac{\partial}{\partial x} \psi_{m2}$$

$$= \frac{j}{4\pi^2} \int\int_{-\infty}^{\infty} \left[\frac{k_y k_{z2}}{\omega\mu_0} \tilde{\psi}_{e2} + k_x \tilde{\psi}_{m2} \right] e^{-j(k_x x + k_y y + k_{z2} z)} dk_x dk_y \,, \tag{A.11}$$

$$H_{z2}(\bar{r}) = \frac{1}{j\omega\mu_0} \left(\frac{\partial^2}{\partial z^2} + k_0^2 \right) \psi_{e2}$$

$$= \frac{-j}{4\pi^2} \int\int_{-\infty}^{\infty} \frac{(k_x^2 + k_y^2)}{\omega\mu_0} \tilde{\psi}_{e2} \, e^{-j(k_x x + k_y y + k_{z2} z)} dk_x dk_y \,. \tag{A.12}$$

Enforcing the boundary conditions at z=0 (dielectric-air interface) specified by Equations (2.8) and (2.9) leads to

$$E_{x1} = E_{x2} \qquad \text{at} \quad z = 0 \tag{A.13}$$

$$E_{y1} = E_{y2} \qquad \text{at} \quad z = 0 \tag{A.14}$$

$$H_{x2} - H_{x1} = J_{sy} \qquad \text{at} \quad z = 0 \tag{A.15}$$

$$-H_{y2} + H_{y1} = J_{sx} \qquad \text{at} \quad z = 0 \,. \tag{A.16}$$

Use of Equations (A.13), (A.1) and (A.7) gives

$$k_y \tilde{\psi}_{e2} + \frac{k_x k_{z2}}{\omega \varepsilon_0} \tilde{\psi}_{m2} = \left[k_y \tilde{\psi}_{e1} - \frac{j}{\omega \varepsilon_0 \varepsilon_r} k_x k_{z1} \tilde{\psi}_{m1} \right] \sin k_{z1} t \quad . \qquad (A.17)$$

Similarly, use of (A.14), (A.2) and (A.8) gives

$$k_x \tilde{\psi}_{e2} - \frac{k_y k_{z2}}{\omega \varepsilon_0} \tilde{\psi}_{m2} = \left[k_x \tilde{\psi}_{e1} + \frac{j}{\omega \varepsilon_0 \varepsilon_r} k_x k_{z1} \tilde{\psi}_{m1} \right] \sin k_{z1} t \quad . \qquad (A.18)$$

Use of (A.15), (A.4), (A.10) and (2.10) gives

$$\left[\frac{k_x k_{z2}}{\omega \mu_0} \tilde{\psi}_{e2} - k_y \tilde{\psi}_{m2} \right] - \left[\frac{j k_x k_{z1}}{\omega \mu_0} \tilde{\psi}_{e1} - k_y \tilde{\psi}_{m1} \right] \cos k_{z1} t = -j \tilde{J}_{sy} \, . \qquad (A.19)$$

Use of (A.16), (A.5), (A.11) and (2.10) gives

$$- \left[\frac{k_y k_{z2}}{\omega \mu_0} \tilde{\psi}_{e2} + k_x \tilde{\psi}_{m2} \right] + \left[\frac{j k_y k_{z1}}{\omega \mu_0} \tilde{\psi}_{e1} + k_x \tilde{\psi}_{m1} \right] \cos k_{z1} t = -j \tilde{J}_{sx} \, . \qquad (A.20)$$

Adding (A.17) multiplied by k_y to (A.18) multiplied by k_x yields

$$(k_x^2 + k_y^2) \tilde{\psi}_{e2} = (k_x^2 + k_y^2) \tilde{\psi}_{e1} \sin k_{z1} t$$

$$\tilde{\psi}_{e2} = \sin k_{z1} t \, \tilde{\psi}_{e1} \quad . \qquad (A.21)$$

Adding (A.17) multiplied by k_x to (A.18) multiplied by $(-k_y)$ yields

$$\frac{(k_x^2 + k_y^2)\, k_{z2}}{\omega\varepsilon_0} \tilde{\psi}_{m2} = \frac{-jk_{z1}}{\omega\varepsilon_0\varepsilon_r}(k_x^2 + k_y^2)\, \tilde{\psi}_{m1} \sin k_{z1}t$$

$$\tilde{\psi}_{m2} = \frac{-jk_{z1}}{\varepsilon_r k_{z2}} \sin k_{z1}t\, \tilde{\psi}_{m1} \quad . \tag{A.22}$$

Adding (A.19) multiplied by k_x to (A.20) multiplied by $(-k_y)$ yields

$$\frac{k_{z2}}{\omega\mu_0}(k_x^2 + k_y^2)\tilde{\psi}_{e2} - j\frac{k_{z1}}{\omega\mu_0}(k_x^2 + k_y^2)\cos k_{z1}t\, \tilde{\psi}_{e1} = j[k_y\tilde{J}_{sx} - k_x\tilde{J}_{sy}]$$

$$\frac{(k_x^2 + k_y^2)}{\omega\mu_0}[k_{z1}\cos k_{z1}t\tilde{\psi}_{e1} + jk_{z2}\tilde{\psi}_{e2}] = k_x\tilde{J}_{sy} - k_y\tilde{J}_{sx} \quad . \tag{A.23}$$

Adding (A.19) multiplied by k_y to (A.20) multiplied by k_x yields

$$-(k_x^2 + k_y^2)\tilde{\psi}_{m2} + (k_x^2 + k_y^2)\tilde{\psi}_{m1}\cos k_{z1}t = -j[k_y\tilde{J}_{sy} + k_x\tilde{J}_{sx}]$$

$$(k_x^2 + k_y^2)[-\tilde{\psi}_{m2} + \tilde{\psi}_{m1}\cos k_{z1}t] = -j[k_y\tilde{J}_{sy} + k_x\tilde{J}_{sx}] \quad . \tag{A.24}$$

Using (A.21) in (A.23) leads to

$$\tilde{\psi}_{e1} = \frac{\omega\mu_0}{(k_x^2 + k_y^2)D_e}[k_x\tilde{J}_{sy} - k_y\tilde{J}_{sx}] \tag{A.25}$$

$$\tilde{\psi}_{e2} = \frac{\omega\mu_0 \sin k_{z1} t}{(k_x^2 + k_y^2) D_e} \left[k_x \tilde{J}_{sy} - k_y \tilde{J}_{sx}\right] \tag{A.26}$$

where

$$D_e = k_{z1} \cos k_{z1} t + j k_{z2} \sin k_{z1} t \tag{A.27}$$

Using (A.22) in (A.24) leads to

$$\tilde{\psi}_{m1} = \frac{-j\varepsilon_r k_{z2}}{(k_x^2 + k_y^2) D_m} \left[k_x \tilde{J}_{sx} + k_y \tilde{J}_{sy}\right] \tag{A.28}$$

$$\tilde{\psi}_{m2} = \frac{-k_{z1} \sin k_{z1} t}{(k_x^2 + k_y^2) D_m} \left[k_x \tilde{J}_{sx} + k_y \tilde{J}_{sy}\right] \tag{A.29}$$

where

$$D_m = \varepsilon_r k_{z2} \cos k_{z1} t + j k_{z1} \sin k_{z1} t \tag{A.30}$$

APPENDIX B

MUTUAL IMPEDANCE BETWEEN TWO PATCH DIPOLE MODES

In this appendix, the exact expressions for the mutual impedance (z_{mn}) between surface patch dipole modes $\bar{J}_m$ and $\bar{J}_n$ on a lossy grounded dielectric slab is presented. The mutual impedance (v_m) between dipole mode $\bar{J}_m$ and the impressed source current $\bar{J}_i$ is also presented. These calculations are essential in solving a microstrip antenna problem by the moment method. z_{mn} and v_m form the elements of the impedance matrix and voltage vector, respectively.

Figure B.1 shows two dipole modes, $\bar{J}_m$ and $\bar{J}_n$, located on the surface of a grounded dielectric slab with parameters μ_o and $\varepsilon_r\varepsilon_o$. The ambient medium is free space with parameters μ_o and ε_o. Mode m is centered with respect to the (x,y) coordinate system. The center of mode n coincides with the origin of the (x',y') system which is displaced from the center of mode m by a position vector (x_o,y_o). The x'-axis is at an angle α with respect to the x-axis.

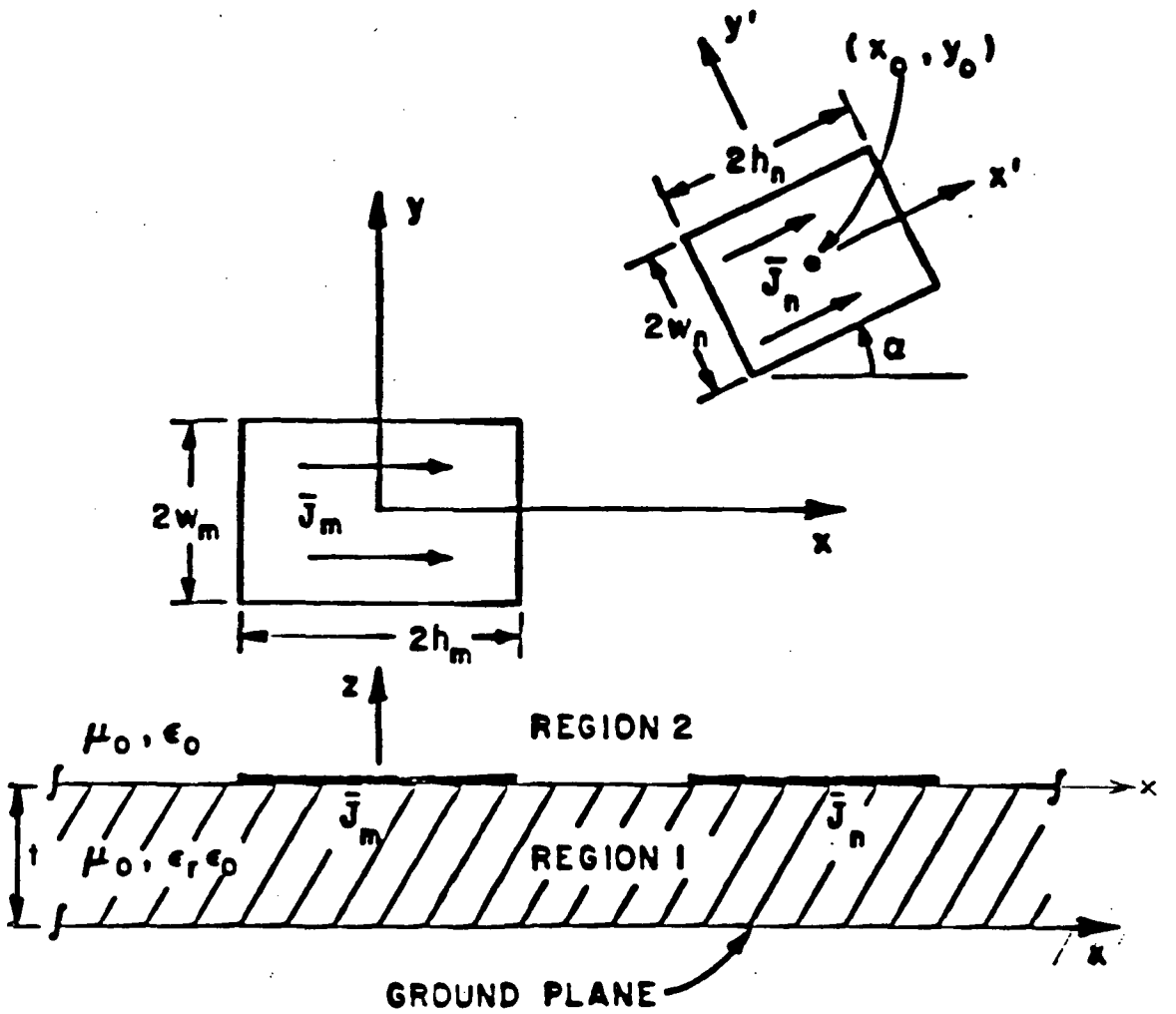

Figure B.1. Two expansion dipole modes on a grounded dielectric slab.

The mutual impedance between modes m and n is given by

$$z_{mn} = - \int_n \bar{E}_m(\bar{r}_o+\bar{r}') \cdot \bar{J}_n(\bar{r}')ds' \tag{B.1}$$

where $\bar{E}_m$ denotes the electric field excited by $\bar{J}_m$, and the integration is over the surface of mode n in the z=0 plane with

$$\bar{r}' = \hat{x}'x' + \hat{y}'y' = \hat{x}(x'\cos\alpha - y'\sin\alpha) + \hat{y}(x'\sin\alpha + y'\cos\alpha) \tag{B.2}$$

$$\bar{r}_o = \hat{x}x_o + \hat{y}y_o \quad . \tag{B.3}$$

Without loss of generality, it is assumed that

$$\bar{J}_m(\bar{r}) = \hat{x}J_{mx}(\bar{r}) + \hat{y}J_{my}(\bar{r}) \tag{B.4}$$

where $\bar{r} = \hat{x}x + \hat{y}y$ and

$$\bar{J}_n(\bar{r}') = \hat{x}'J_{nx'}(\bar{r}') + \hat{y}'J_{ny'}(\bar{r}') \quad . \tag{B.5}$$

It then follows from (2.17), (2.18), (2.24) and (2.26) that, at z=0,

$$E_{mx}(\bar{r}_o+\bar{r}') = \frac{j}{4\pi^2} \iint_{-\infty}^{\infty} [k_y \tilde{\psi}_{e2} + \frac{k_x k_{z2}}{\omega\varepsilon_0} \tilde{\psi}_{m2}] e^{-j(k_x x_o + k_y y_o)}$$

$$\cdot e^{-j\phi(x',y',\alpha)} \, dk_x dk_y \tag{B.6}$$

$$E_{my}(\bar{r}_o+\bar{r}') = \frac{-j}{4\pi^2} \iint_{-\infty}^{\infty} [k_x \tilde{\psi}_{e2} - \frac{k_y k_{z2}}{\omega\varepsilon_0} \tilde{\psi}_{m2}] e^{-j(k_x x_o + k_y y_o)}$$

$$\cdot e^{-j\phi(x',y',\alpha)} \, dk_x dk_y \qquad (B.7)$$

where

$$k_{z2} = \sqrt{k_o^2 - k_x^2 - k_y^2} \quad , \; Imk_{z2} < 0, \; Rek_{z2} > 0 \quad , \qquad (B.8)$$

$$\phi(x',y',\alpha) = x'(k_x \cos\alpha + k_y \sin\alpha) + y'(-k_x \sin\alpha + k_y \cos\alpha) \quad , \qquad (B.9)$$

$$\tilde{\psi}_{e2} = \frac{\omega\mu_0 \sin k_{z1} t}{(k_x^2+k_y^2) D_e} [k_x \tilde{J}_{my} - k_y \tilde{J}_{mx}] \quad , \qquad (B.10)$$

$$\tilde{\psi}_{m2} = \frac{-k_{z1} \sin k_{z1} t}{(k_x^2+k_y^2) D_m} [k_x \tilde{J}_{mx} + k_y \tilde{J}_{my}] \quad , \qquad (B.11)$$

$$k_{z1} = \sqrt{\varepsilon_r k_o^2 - k_x^2 - k_y^2} \quad , \qquad (B.12)$$

$$D_e = k_{z1} \cos k_{z1} t + j k_{z2} \sin k_{z1} t \quad , \qquad (B.13)$$

$$D_m = \varepsilon_r k_{z2} \cos k_{z1} t + j k_{z1} \sin k_{z1} t \quad , \qquad (B.14)$$

$$\tilde{J}_{mx}(k_x,k_y) = \iint_{-\infty}^{\infty} J_{mx}(x,y) e^{j(k_x x + k_y y)} dxdy \quad , \qquad (B.15)$$

and

$$\tilde{J}_{my}(k_x,k_y) = \iint_{-\infty}^{\infty} J_{my}(x,y)e^{j(k_x x+k_y y)}dxdy \quad . \tag{B.16}$$

Also one may note that the tangential component of $\bar{E}_m(\bar{r}_o+\bar{r}')$ on the surface of mode n is given by

$$\begin{aligned}\bar{E}_m^t(\bar{r}_o+\bar{r}') &= \hat{x}E_{mx}(\bar{r}_o+\bar{r}') + \hat{y}E_{my}(\bar{r}_o+\bar{r}') \\ &= \hat{x}'[E_{mx}(\bar{r}_o+\bar{r}')\cos\alpha + E_{my}(\bar{r}_o+\bar{r}')\sin\alpha] \\ &+ \hat{y}'[-E_{mx}(\bar{r}_o+\bar{r}')\sin\alpha + E_{my}(\bar{r}_o+\bar{r}')\cos\alpha] \quad .\end{aligned} \tag{B.17}$$

Combining (B.1), (B.5) and (B.17) yields

$$\begin{aligned}z_{mn} = -\int_{-h_n}^{h_n}\int_{-w_n}^{w_n} &\{[E_{mx}(\bar{r}_o+\bar{r}')\cos\alpha + E_{my}(\bar{r}_o+\bar{r}')\sin\alpha]J_{nx'}(x',y') \\ &+ [-E_{mx}(\bar{r}_o+\bar{r}')\sin\alpha + E_{my}(\bar{r}_o+\bar{r}')\cos\alpha]J_{ny'}(x',y')\}dy'dx' \quad .\end{aligned} \tag{B.18}$$

Next let

$$\begin{aligned}\tilde{J}_{nx'}(k_x,k_y,\alpha) &= \int_{-h_n}^{h_n}\int_{-w_n}^{w_n} J_{nx'}(x',y')e^{-j\phi(x',y',\alpha)}dy'dx' \\ &= \int_{-h_n}^{h_n}\int_{-w_n}^{w_n} J_{nx'}(x',y') \\ &\cdot e^{-j[x'(k_x\cos\alpha+k_y\sin\alpha)+y'(-k_x\sin\alpha+k_y\cos\alpha)]}dy'dx'\end{aligned} \tag{B.19}$$

and

$$\tilde{J}_{ny'}(k_x,k_y,\alpha) = \int_{-h_n}^{h_n}\int_{-w_n}^{w_n} J_{ny'}(x',y')e^{-j\phi(x',y',\alpha)}dy'dx'$$

$$= \int_{-h_n}^{h_n}\int_{-w_n}^{w_n} J_{ny'}(x',y')$$

$$\cdot e^{-j[x'(k_x\cos\alpha+k_y\sin\alpha)+y'(-k_x\sin\alpha+k_y\cos\alpha)]}dy'dx' \quad . \qquad (B.20)$$

Use of (B.6), (B.7), (B.19) and (B.20) in (B.18) leads to

$$z_{mn} = -\frac{j}{4\pi^2}\int_{-\infty}^{\infty}\int \Bigg[\Bigg[\Bigg[(k_y\tilde{\psi}_{e2} + \frac{k_xk_{z2}}{\omega\varepsilon_0}\tilde{\psi}_{m2})\cos\alpha$$

$$- (k_x\tilde{\psi}_{e2} - \frac{k_yk_{z2}}{\omega\varepsilon_0}\tilde{\psi}_{m2})\sin\alpha\Bigg]\tilde{J}_{nx'}(k_x,k_y,\alpha)$$

$$- \Bigg[(k_y\tilde{\psi}_{e2} + \frac{k_xk_{z2}}{\omega\varepsilon_0}\tilde{\psi}_{m2})\sin\alpha + (k_x\tilde{\psi}_{e2} - \frac{k_yk_{z2}}{\omega\varepsilon_0}\tilde{\psi}_{m2})\cos\alpha\Bigg]$$

$$\cdot \tilde{J}_{ny'}(k_x,k_y,\alpha)\Bigg] e^{-j(k_xx_o + k_yy_o)}dk_xdk_y \quad . \qquad (B.21)$$

z_{mn} in Equation (B.21) represents the most general expression for the mutual impedance between two rectangular dipole modes on a planar grounded dielectric slab.

Referring to Figure B.2, the mutual impedance between dipole mode J_m and impressed source $\bar{J}_i$ is defined as

$$V_m = \int_V \bar{E}_m(\bar{r}) \cdot \bar{J}_i(\bar{r}) dv \quad . \tag{B.22}$$

Since source $\bar{J}_i$ can be reasonably modeled as a vertical filament of constant current inside the dielectric, it is represented by

$$\bar{J}_i(\bar{r}) = \hat{z} I_i \delta(x-x_f)\delta(y-y_f) \quad , \; -\infty<x,y<\infty \; , \; -t \leq z \leq 0 \tag{B.23}$$

where I_i is the magnitude of the feed current and (x_f,y_f) denotes the filament location in the x-y plane, with respect to the center of mode m.

Making use of (2.13), one can write

$$E_{mz}(\bar{r}) = \frac{-j}{4\pi^2} \iint_{-\infty}^{\infty} \frac{(k_x^2+k_y^2)}{\omega\varepsilon_0\varepsilon_r} \tilde{\psi}_{m1} \, e^{-j(k_x x+k_y y)} \cos k_{z1}(z+t) dk_x dk_y \quad . \tag{B.24}$$

Inserting (B.23) and (B.24) into (B.22) and carrying out the volume integration gives

$$V_m = \frac{-jI_i}{4\pi^2} \iint_{-\infty}^{\infty} \frac{(k_x^2+k_y^2)}{\omega\varepsilon_0\varepsilon_r k_{z1}} \tilde{\psi}_{m1} \, e^{-j(k_x x_f+k_y y_f)} \sin k_{z1} t \, dk_x dk_y \quad . \tag{B.25}$$

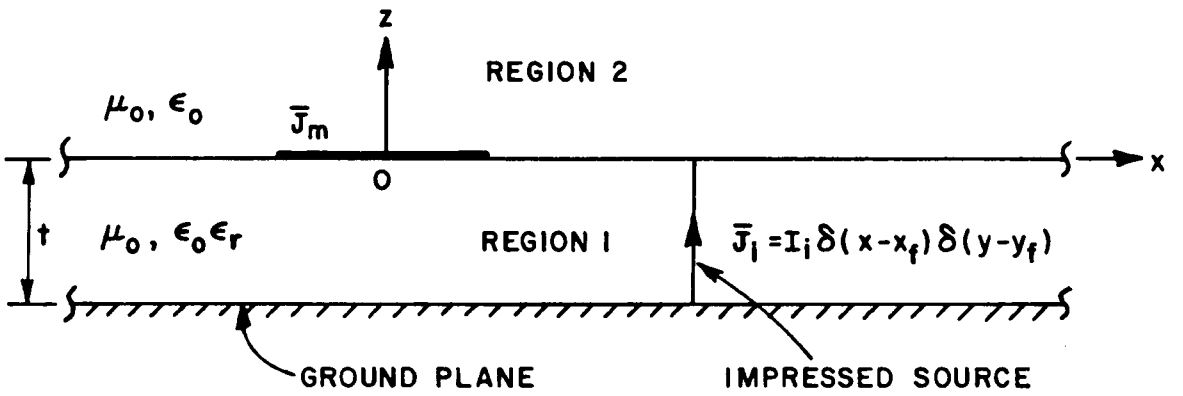

Figure B.2. A dipole mode $\bar{J}_m$ and an impressed current source $\bar{J}_i$.

In both (B.24) and (B.25)

$$\tilde{\psi}_{m1} = - \frac{j\varepsilon_r k_{z2}}{(k_x^2+k_y^2)D_m} [k_x \tilde{J}_{mx} + k_y \tilde{J}_{my}] \quad . \tag{B.26}$$

APPENDIX C

PATCH DIPOLE MODES

In this appendix, the specific patch dipole modes and their corresponding Fourier transforms are presented. In using the moment method to analyze the performance of a microstrip patch antenna at higher order resonant frequencies, it is appropriate to employ the entire functions as the expansion dipole modes. On rectangular patches, the $\hat{x}$ polarized current modes will have the form

$$\bar{J}_{mn}(x,y) = \hat{x} \left\{ \sin \frac{m\pi}{2L_x} (x+L_x) \cos \frac{n\pi}{2L_y} (y+L_y) \right\} \quad , \qquad (C.1)$$

where $m=1,2,3,\ldots$, $n=0,1,2,3,\ldots$, $-L_x < x < L_x$ and $-L_y < y < L_y$ with $L_x \neq 0 \neq L_y$. It should note that the dipole modes $\bar{J}_{mn}$ have double subscripts instead of single subscripts which appear in Chapters 2 and 3. The double subscripts allow the modes to vary as simusoidal functions in both the x-and y-coordinates.

It is easy to show that the Fourier transforms of $\bar{J}_{mn}$ assume the following forms:

$$\tilde{J}_{mn}(k_x,k_y) = \int_{-L_y}^{L_y} \int_{-L_x}^{L_x} \bar{J}_{mn}(x,y)\, e^{j(k_x x+k_y y)}\, dxdy$$

$$= \hat{x} X_m(k_x)\, Y_n(k_y) \quad , \tag{C.2}$$

where

$$X_m(k_x) = \begin{cases} \dfrac{-\dfrac{m\pi}{L_x}\cos k_x L_x}{k_x^2\left[1-\left(\dfrac{m\pi}{2L_x k_x}\right)^2\right]} & , \quad m=1,3,5,\ldots \\ \dfrac{\dfrac{jm\pi}{L_x}\sin k_x L_x}{k_x^2\left[1-\left(\dfrac{m\pi}{2L_x k_x}\right)^2\right]} & , \quad m=2,4,6,\ldots \end{cases} \tag{C.3}$$

and

$$Y_n(k_y) = \begin{cases} \dfrac{j2\cos k_y L_y}{k_y\left[1-\left(\dfrac{n\pi}{2L_y k_y}\right)^2\right]} & , \quad n=1,3,5,\ldots \\ \dfrac{2\sin k_y L_y}{k_y\left[1-\left(\dfrac{n\pi}{2L_y k_y}\right)^2\right]} & , \quad n=0,2,4,\ldots \end{cases} \tag{C.4}$$